Heat Transfer Criteria of a Tubular Solar Collector – The Effect of Reversing the Flow Pattern on Collector Performance

F. L. Lansing
DSN Engineering Section

A new evacuated tubular solar collector has been selected for further investigation for the application of Goldstone energy conservation projects. This article presents briefly the exact heat transfer analysis of this two-pass-flow collector in an effort to determine the difference in performance characteristics with two different flow patterns. The results from this analysis are not only the determination of the collected heat rate and the temperature profiles at each cross section but also the prediction of the maximum attainable fluid temperature at zero flow rate in both cases.

I. Introduction

Part of the updated technology in energy conservation measures, using solar-assisted equipment, is the development of a new evacuated tubular two-pass-flow solar collector. This is a prospective candidate collector with a relatively higher thermal performance than the flat-plate type. The collector has been selected by the DSN Engineering Section for further theoretical and practical investigation for application in Goldstone energy conservation projects.

Limited laboratory measurements were the only data available for the performance of this collector. The latest attempt (Ref. 1) at NASA Lewis Research Center using a solar simulator and an analogous one-pass-flow tubular collector was found insufficient to provide the relevant performance characteristics of the actual two-pass-flow tubular collector. The common analysis procedure (Ref. 2) of assuming an overall, one-directional heat loss to the surroundings in a flat-plate collector expression is no longer adequate for exact performance analysis with two different kinds of flow patterns. This suggested the need for exact heat transfer and flow analyses as an essential step in the determination of performance characteristics over wide ranges of irradiancies, fluid flow rates, inlet fluid temperatures and ambient conditions. This article presents the steps and results of these analyses.

II. Collector Description and Flow Patterns

The tubular collector, as shown schematically in Figs. 1a and 2a, is composed of three all-glass concentric tubes, namely, a feeder tube, an absorber tube and a cover tube. The annulus space between the absorber and cover tubes is evacuated to such a low pressure ($\sim 10^{-4}$ torr) that convection and conduction losses are negligible. The absorber tube surface is coated with a selective material which minimizes outward long-wave radiation losses. In flow pattern (1), as shown in Fig. 1, the fluid, normally water, starts from the inlet section of the feeder tube and absorbs some of the useful solar energy along its path, thus raising its temperature. At the closed end of the collector, the fluid reverses its direction and passes in the annulus spacing between the feeder and absorber tubes. The temperature distribution along one streamline is as shown in Fig. 1b.

In flow pattern (2), as shown in Fig. 2, the fluid path is reversed from the above. It starts from one end of the collector through the annulus spacing, turns around at the closed end, and then leaves from the other end from the feeder tube. Both flow patterns (1) and (2) alternate, in each collector module, as shown in Fig. 3.

For more irradiancy augmentation, the set of collectors is mounted, with lateral spaces separating them from each other with a highly reflective back reflector, as shown in Fig. 4. This increases the overall irradiancy (Refs. 1 and 2) by as much as 64 percent at normal solar incidence.

III. Analysis

For a segment of the collector of length dx at steady-state conditions, the heat flux is divided as shown in Fig. 5, where

dQ_1 = the total irradiation on the cover tube from all sides (including irradiancies from the back reflector and reflections from adjacent collectors).

dQ_2 = the energy absorbed by the absorber tube (including absorption from multiple reflections within the evacuated space).

dQ_3 = the total outward reflection loss from all sides of the cover tube.

dQ_4 = the energy absorbed by the cover tube (including absorption from multiple reflections within the evacuated space).

dQ_5 = the long-wave radiation exchange between the cover and absorber tubes. (This is absorbed by the cover, thus raising its temperature.)

dQ_6 = the heat transfer to fluid (2) in the annulus pass from the absorber tube surface.

dQ_7 = the augmented radiation and convection loss between the cover tube and ambient air and sky.

dQ_8 = the heat transfer to fluid (1) in the feeder tube.

dQ_9 = the sensible heat gain to fluid (2) in the annulus pass.

For both flow patterns, at steady state, the heat balance of the absorber tube alone can be expressed as

$$dQ_2 - dQ_5 - dQ_6 = 0 \tag{1}$$

and the heat balance of the cover tube alone can be written as

$$dQ_4 + dQ_5 - dQ_7 = 0 \tag{2}$$

By eliminating the cover tube temperature, $T_3(x)$, and the absorber tube temperature, $T_s(x)$, from the heat balance equations for fluids (1) and (2), the problem is reduced to the solution of the two simultaneous differential equations, as follows:

$$\left.\begin{aligned} &\frac{dT_1(x)}{dx} + K_1 T_1(x) = K_1 T_2(x) \\ -&\frac{dT_2(x)}{dx} + K_3 T_2(x) = K_1 T_1(x) + K_4 \end{aligned}\right\} \text{for flow pattern (1)} \tag{3}$$

and

$$\left.\begin{aligned} -&\frac{dT_1(x)}{dx} + K_1 T_1(x) = K_1 T_2(x) \\ &\frac{dT_2(x)}{dx} + K_3 T_2(x) = K_1 T_1(x) + K_4 \end{aligned}\right\} \text{for flow pattern (2)} \tag{4}$$

where K_1, K_2, K_3, and K_4 are constants determined from the steady-state thermal analysis, and $T_1(x)$, $T_2(x)$ are the fluid temperatures in passes (1) and (2), respectively, at a distance x from the inlet section.

IV. Boundary Conditions

(1) $T_1(x) = T_2(x)$ at $x = L$ for both flow patterns (1) and (2)

(2) $T_1(x) = T_1(0)$ at $x = 0$ for flow pattern (1)

(3) $T_2(x) = \overline{T}_2(0)$ at $x = 0$ for flow pattern (2)

The temperature distribution $T_1(x)$, $T_2(x)$ of the fluid for pattern (1) or $\overline{T}_1(x)$, $\overline{T}_2(x)$ for pattern (2) can now be determined.

For flow pattern (1), and at the inlet section ($x = 0$), the temperature of the fluid leaving the collector $T_2(0)$ is given by

$$T_2(0) = T_1(0) + \left\{\left[T_1(0) - \frac{K_4}{K_3 - K_1}\right]\frac{s_1}{K_1} \times \left[\frac{1 - \exp[(s_1 - s_2)L]}{1 - \frac{s_1}{s_2}\exp[(s_1 - s_2)L]}\right]\right\} \quad (5)$$

where s_1 and s_2 are the roots of the quadratic auxiliary equation:

$$s_{1,2}^2 - (K_3 - K_1)s_{1,2} - K_1(K_3 - K_1) = 0 \quad (6)$$

For flow pattern (2) and at the inlet section ($x = 0$), the temperature of the fluid leaving the collector $\overline{T}_1(0)$ is given by

$$\overline{T}_1(0) = \overline{T}_2(0) - \left\{\left[\overline{T}_2(0) - \frac{K_4}{(K_3 - K_1)}\right]\frac{\overline{s}_1}{K_1} \times \left[\frac{1 - \exp[(\overline{s}_1 - \overline{s}_2)L]}{(1 - \frac{\overline{s}_1}{\overline{s}_2}\exp[(\overline{s}_1 - \overline{s}_2)L] + \frac{\overline{s}_1}{K_1}(\exp[(\overline{s}_1 - \overline{s}_2)L] - 1)}\right]\right\} \quad (7)$$

where $\overline{s}_1$ and $\overline{s}_2$ are the roots of the quadratic auxiliary equation:

$$\overline{s}_{1,2}^2 + (K_3 - K_1)\overline{s}_{1,2} - K_1(K_3 - K_1) = 0 \quad (8)$$

From Eqs. (6) and (8), it can be proved that the roots $\overline{s}_1$ and $\overline{s}_2$ are related to the roots s_1, s_2 by

$$\left.\begin{aligned} \overline{s}_1 &= -s_1 \\ \overline{s}_2 &= -s_2 \\ K_1(s_1 s_2) + (s_1 + s_2) &= 0 \end{aligned}\right\} \quad (9)$$

Substituting Eq. (9) in Eq. (7) will show that the expressions, Eq. (5) and Eq. (7), for the leaving fluid temperature in both fluid patterns are identical.

The results from this analysis are the determination of the collected heat rate and also the temperature distribution of the fluid as it flows in each pass in addition to the absorber and cover temperatures.

V. Maximum Fluid Temperature for Zero Flow Rate

The constants K_1, K_2, K_3, K_4, s_1, s_2, $\overline{s}_1$, and $\overline{s}_2$ are found to approach an infinity value as the mass flow rate approaches zero. However, their quotients have finite values independent of the fluid rate. Accordingly, it is always possible to find finite values for the ratios s_1/s_2, $\overline{s}_1/\overline{s}_2$, $K_4/(K_3 - K_1)$, $\overline{s}_1/K_1$, and s_1/K_1. Using L'Hopital's rule for indefinite quantities, the maximum fluid temperature, $T_2(0)$, for both flow patterns will be the limiting value, from Eq. (5) or Eq. (7), as the mass flow rate approaches zero. This is given by

$$[T_2(0)]_{\max} = T_1(0) + \left[T_1(0) - \frac{K_4}{K_3 - K_1}\right]\frac{s_2}{K_1} \quad (10)$$

VI. Numerical Example

The following numerical example will show the difference in performance between the two flow patterns of the tubular solar collector. The data were arbitrarily abstracted to be as close as possible to actual running conditions. However, the conclusions may be generalized at any other relevant conditions.

Irradiation with normal incidence to back reflector

Inlet water temperature $T_1(0)$ in pattern (1) or $T_2(0)$ in pattern (2)	70°C
Ambient temperature T_0	30°C

Sky temperature	4°C
Irradiation intensity	0.75 kW/m^2
Tube length	1.067 m
Feeder tube diameter	0.029 m
Absorber tube diameter	0.041 m
Cover tube diameter	0.51 m
Glass refraction index	1.526
Cover tube transmissivity	0.91
Cover tube emissivity	0.90
Absorber tube absorptivity	0.85
Absorber tube emissivity	0.10
Mass flow rate	5 kg/hr
Area of back reflector/ single collector	0.10645 m^2
Distance between two consecutive cover tubes	0.05 m
Distance between cover tubes and back reflector	0.05 m
Wind speed	11 km/hr
Water specific heat	11.634 × 10^{-4} kWh/kg K

A. Collector Efficiency

The relevant constants K_1, K_2, K_3, and K_4 were calculated and given as

$$K_1 = 0.88532\ \text{m}^{-1} \qquad K_3 = 0.90242\ \text{m}^{-1}$$

$$K_2 = 2.50333\ \text{m}^{-1} \qquad K_4 = 13.44064\ \text{K/m}$$

The roots of Eq. (6) were given by

$$s_1 = +0.13189\ \text{m}^{-1} \qquad s_2 = -0.11479\ \text{m}^{-1}$$

and those of Eq. (8) were given by

$$\overline{s_1} = -0.13189\ \text{m}^{-1} \qquad \overline{s_2} = +0.11479\ \text{m}^{-1}$$

Substituting in Eqs. (5) and (7), the leaving temperature $T_2(0)$ in flow pattern (1) or $\overline{T}_1(0)$ in flow pattern (2) was found to be the same in both cases and equal to 350.96 K (77.96°C).

The instantaneous collector efficiency, based on the irradiation on the back reflector, was then calculated as

$$\text{collector efficiency} = \frac{(77.96 - 70) \times 5 \times 11.634 \times 10^{-4}}{0.75 \times 0.10645} = 58\%$$

for both flow patterns.

B. Temperature Distribution

For this example, the absolute temperature of the fluid in the feeder tube $T_1(x)$, the fluid in the annulus spacing $T_2(x)$, the absorber surface temperature $T_s(x)$ and the cover surface temperature $T_3(x)$ were given by

flow pattern (1)

$$T_1(x) = 786.026 - 177.572 \exp(0.13189x) - 265.454 \exp(-0.11479x)\ \text{K}$$

$$T_2(x) = 786.026 - 204.025 \exp(0.13189x) - 231.036 \exp(-0.11479x)\ \text{K}$$

$$T_s(x) = 5.369 + 0.993\, T_2(x)\ \text{K}$$

$$T_3(x) = 290.47 + 0.026\, T_s(x)\ \text{K}$$

flow pattern (2)

$$\overline{T}_1(x) = 786.026 - 231.036 \exp(-0.13189x) - 204.025 \exp(0.11479x)\ \text{K}$$

$$\overline{T}_2(x) = 786.026 - 265.454 \exp(-0.13189x) - 177.572 \exp(0.11479x)\ \text{K}$$

$$\overline{T}_s(x) = 5.369 + 0.993\, T_2(x)\ \text{K}$$

$$\overline{T}_3(x) = 290.47 + 0.026\, T_s(x)\ \text{K}$$

The temperature profile was plotted in Fig. 6 for each flow pattern. It is obvious that in the case of flow pattern (2), the fluid in the annulus spacing at the closed end ($x = L$) will reach a higher temperature than that in flow pattern (1). This is due to the augmenting heat transfer from solar irradiancy and from the relatively hotter fluid in the feeder tube.

C. Maximum Temperature for Zero Flow Rate

Since the running conditions in this example were initially characterized by a slow flow rate (5 kg/hr), it was reasonable to assume, without great loss of accuracy, that

the convective and radiative heat transfer coefficients do not change appreciably by further decrease of the flow rate. Accordingly, the ratio s_2/K_1 approaches -0.12965 and $K_4/(K_3 - K_1)$ approaches 786.026 K as the mass flow rate approaches zero. The limit of the temperature difference $[T_2(0) - T_1(0)]$ from Eq. (10) approaches 57.44°C as the mass flow rate approaches zero. This means that it is possible for the previous operating conditions and both flow patterns to reach a leaving fluid temperature of 127.44°C by one collector with an extremely slow flow rate.

VII. Performance Comparison

The results of the above steady-state analysis can be summarized as follows:

(1) The working fluid with different flow patterns (1) and (2) in the tubular solar collector yields the same value of temperature difference only across the open end of the collector. This result is a useful tool in simplifying the collector module performance by adopting *one* analytical expression for both flow patterns between inlet and leaving fluid temperatures.

(2) The design of selective coating and its durability should take into consideration the larger thermal gradient and the higher absorber tube temperature in flow pattern (2) compared with that in flow pattern (1). The relatively faster degradation of the coating of flow pattern (2) compared with that of flow pattern (1) will affect the maintenance costs.

Having established an analytic expression for collector performance enables the study of future topics. Examples of these topics are the effects of introducing different types of working fluids or setting different collector dimensions.

References

1. Simon, F., *Solar Collector Performance Evaluation with the NASA-Lewis Solar Simulator — Results for an All-Glass-Evacuated Tubular Selectivity Coated Collector with a Diffuse Reflector*, NASA Technical Memorandum NASA TM X-71695, 1975.

2. Beekly, D. C., and Mather, G. R., "Analysis and Experimental Tests of High Performance Tubular Solar Collector," Presented at Int. Solar Energy Society Meeting, UCLA, August 1975.

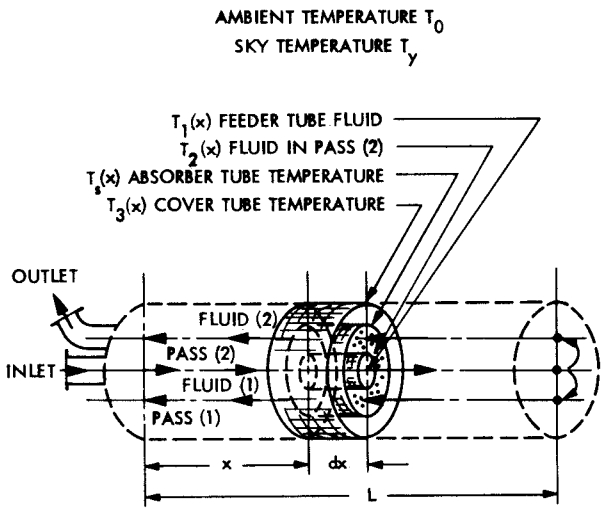

Fig. 1a. Collector configuration (flow pattern 1)

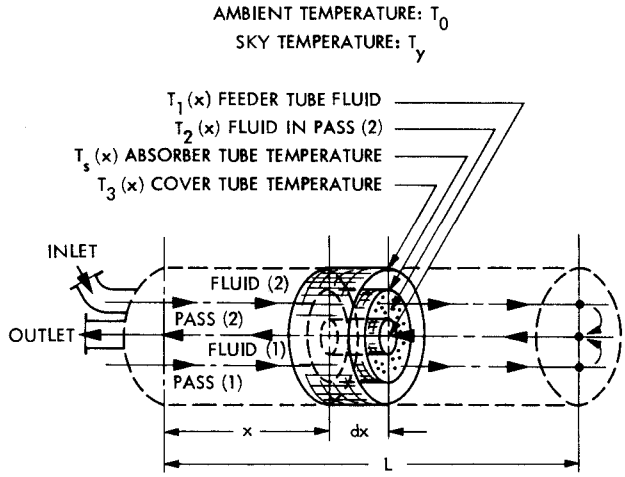

Fig. 2a. Collector configuration (flow pattern 2)

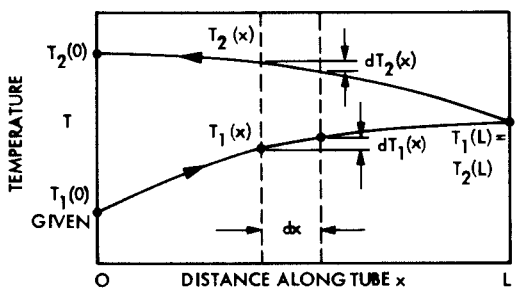

Fig. 1b. Temperature distribution along one collector (flow pattern 1)

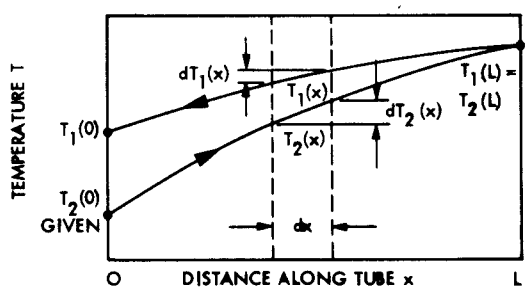

Fig. 2b. Temperature distribution along one collector (flow pattern 2)

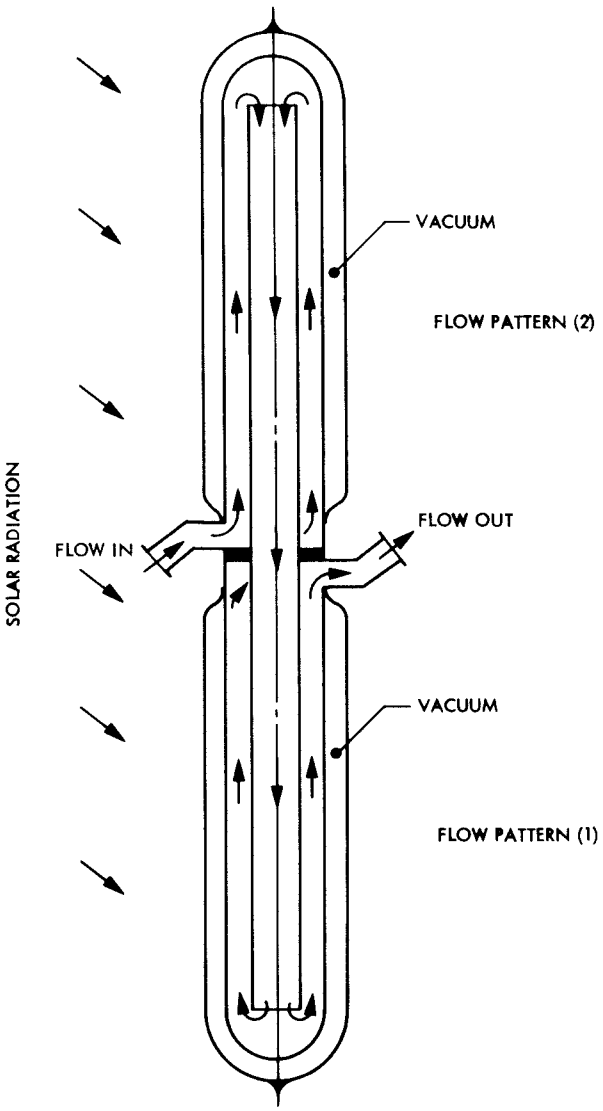

Fig. 3. Two collector tubes in series

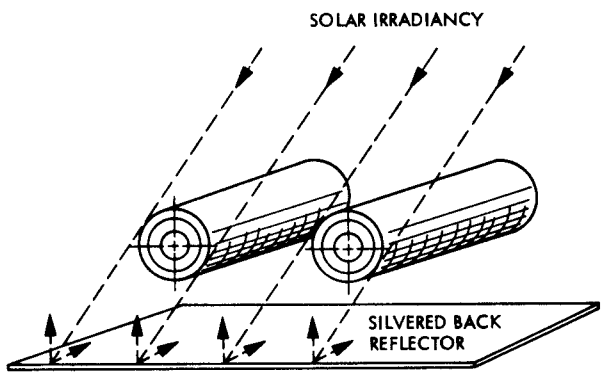

Fig. 4. Arrangement of two collectors with a flat back reflector

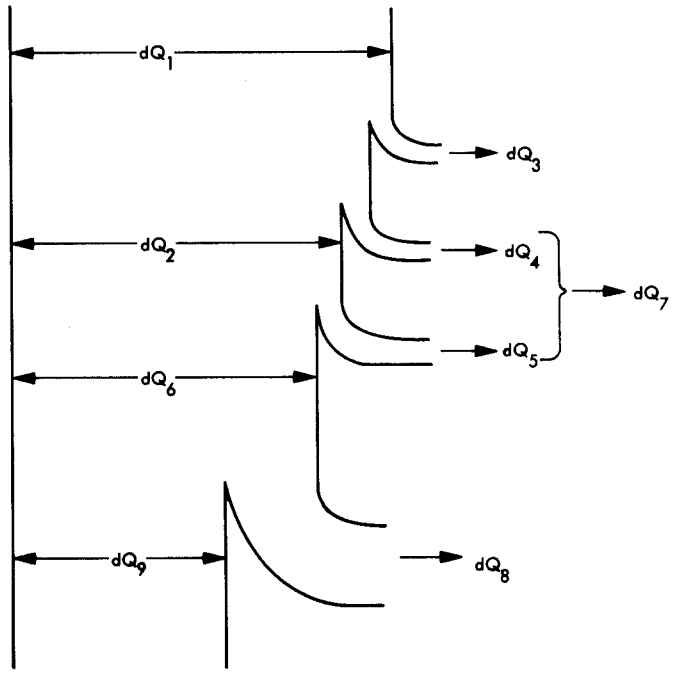

Fig. 5. Sankey diagram for the two-pass-flow collector

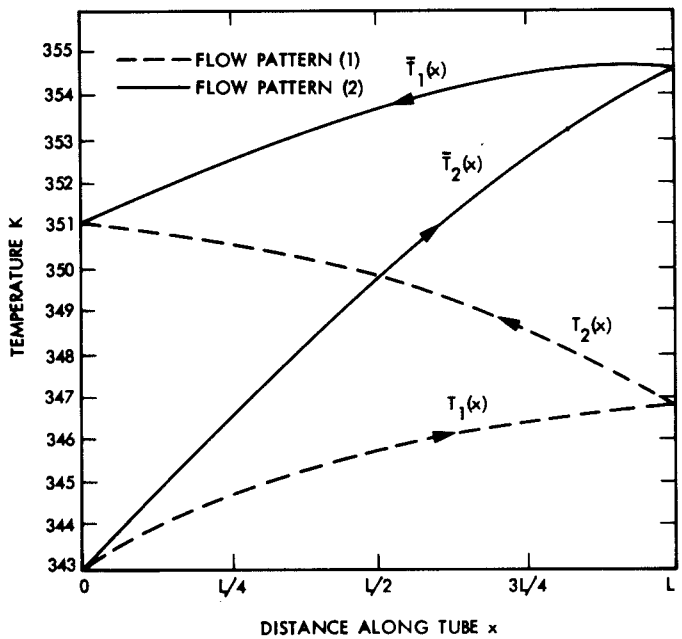

Fig. 6. Temperature distribution along a streamline with a flow pattern (1) and (2)